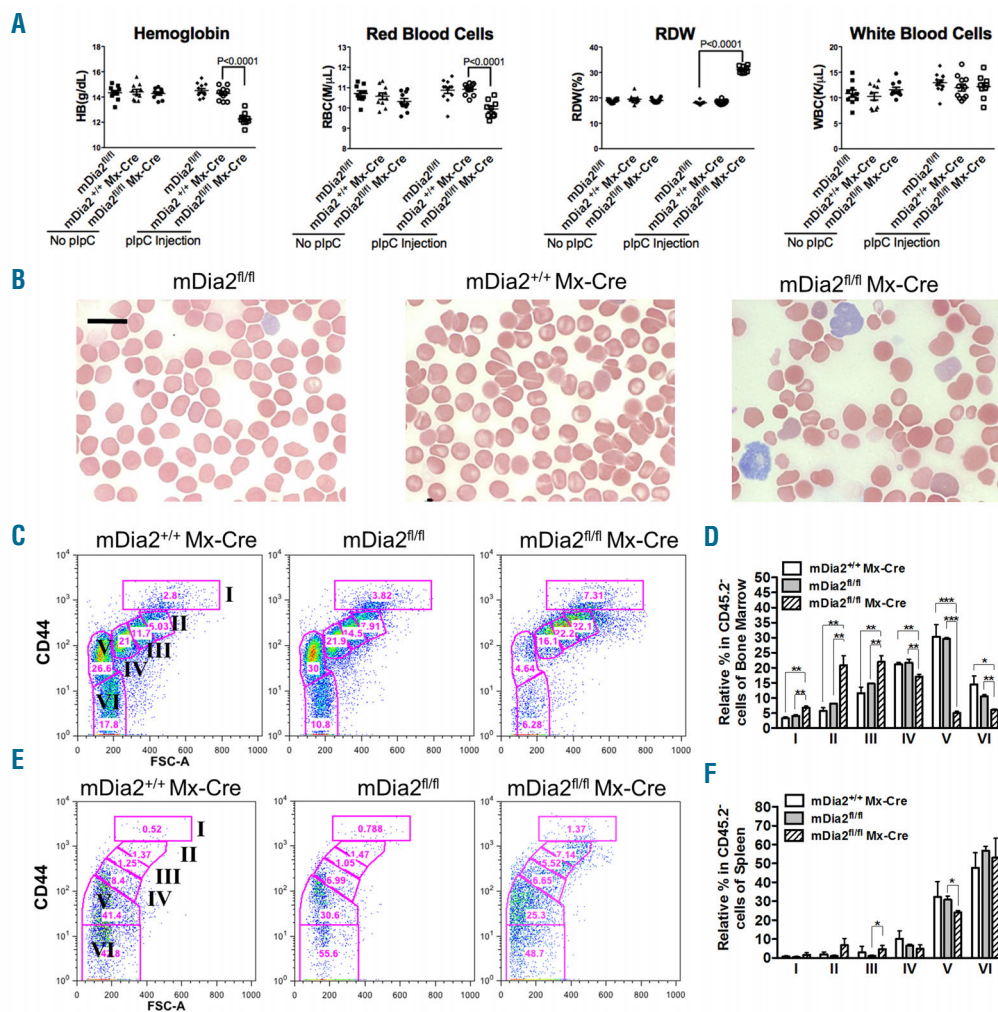


## Ineffective erythropoiesis caused by binucleated late-stage erythroblasts in mDia2 hematopoietic specific knockout mice

The generation of mature red blood cells is initiated from the commitment of hematopoietic stem cells to erythroid progenitors, which is followed by their differentiation to a series of morphologically recognizable erythroblasts.<sup>1</sup> At the end of terminal erythropoiesis, the highly condensed nucleus migrates to one side of the cytoplasm of orthochromatic erythroblast, which is followed by the unique enucleation process producing reticulocytes and mature red blood cells.<sup>2-4</sup> Our previous study demonstrated that mDia2, which belongs to the mDia formin protein family,<sup>5</sup> is a downstream effector protein of Rac GTPases regulating late-stage terminal erythropoiesis, especially enucleation.<sup>6</sup> Herein we generated conditional mDia2 knockout mouse models to reveal the

roles of mDia2 in adult erythropoiesis. The conditional mDia2 knockout mouse models utilized an mDia2 targeting allele with exons 10 and 11 floxed. The LacZ and neomycin cassettes were flanked by FRT to be removed by FLP recombinase (*Online Supplementary Figure S1A*). We first crossed mDia2<sup>fl/fl</sup> mice with E2A-Cre transgenic mice to generate whole body mDia2 knockout mice. The depletion of mDia2 mRNA and protein were confirmed by real-time PCR and Western blot assays (*Online Supplementary Figure S1B and S1C*, respectively). As previously reported,<sup>7</sup> mDia2<sup>fl/fl</sup>E2A-Cre mice were never generated alive (*Online Supplementary Figure S1D*). We found that the mDia2 knockout embryos die in uterus at approximately embryonic day 12.5 (E12.5) (*Online Supplementary Figure S1E*). This demonstrates that mDia2 is essential for embryonic development, which compromises the study of the roles of mDia2 *in vivo* in adults.

To determine the specific roles of mDia2 in adult erythropoiesis, we crossed mDia2<sup>fl/fl</sup> mice with Mx-Cre trans-



**Figure 1. Hematopoietic specific mDia2 knockout mice develop anemia and ineffective erythropoiesis.** (A) Hemoglobin, peripheral red blood cell count, red blood cell distribution width (RDW) and absolute white blood cell count from age matched control (mDia2<sup>fl/fl</sup>, N=11 and mDia2<sup>+/+</sup>Mx-Cre, N=11) and hematopoietic specific knockout (mDia2<sup>fl/fl</sup>Mx-Cre, N=8) mice, 10 weeks post the first poly-IC injection. (B) Wright-Giemsa stains of peripheral blood smears from indicated mice. Scale bars: 15  $\mu$ m. (C-F) Flow cytometric analysis of CD44 and forward scatter levels of CD45 negative erythroblasts from the bone marrow (C) and spleen (E) of indicated mice. Populations I-VI were defined as proerythroblasts, basophilic erythroblasts, polychromatic erythroblasts, orthochromatic erythroblasts, reticulocytes, and red blood cells, respectively<sup>8</sup>. Statistical analysis of (C) and (E) were shown in (D) and (F), respectively. N=3 in each group. \* $P < 0.05$ ; \*\* $P < 0.005$ ; \*\*\* $P < 0.0005$ .

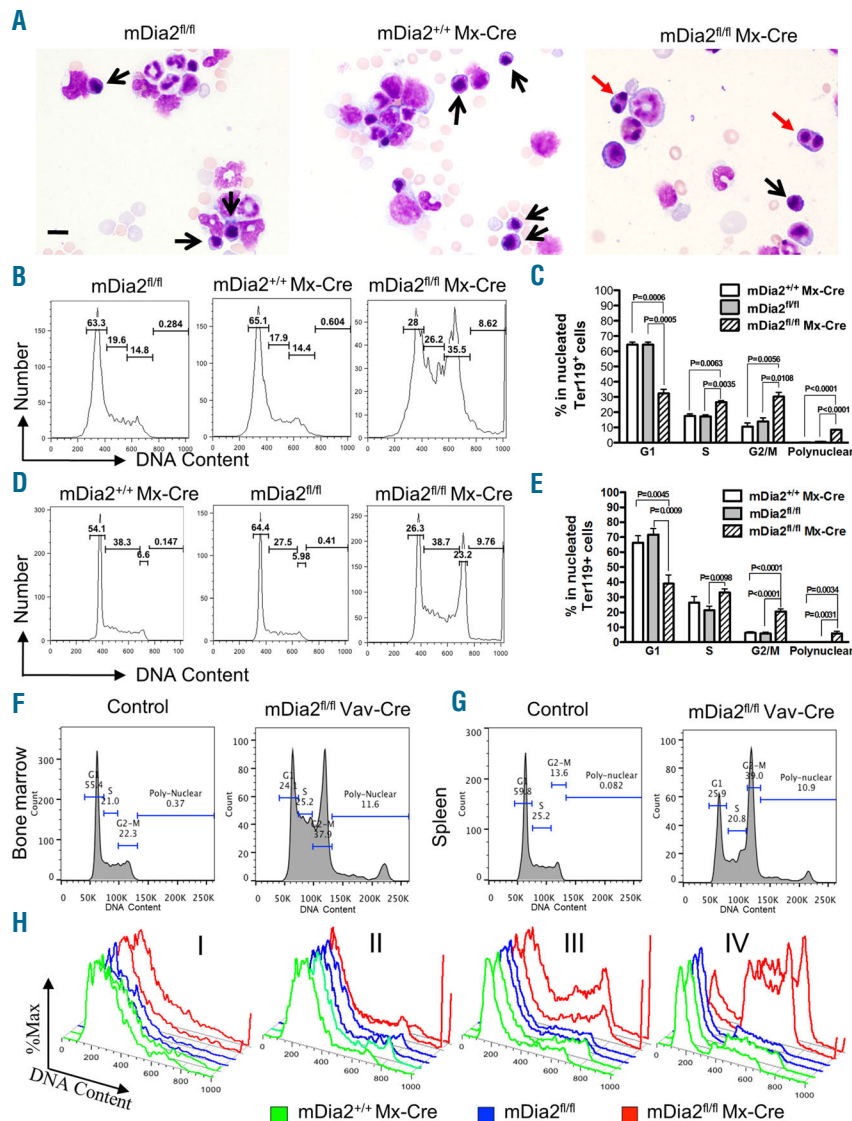


**Figure 2. Loss of mDia2 causes binucleated late-stage erythroblasts in adult mice.**

(A) Wright-Giemsa stains of bone marrow smears from indicated mice. Black and red arrows indicate normal and binucleated erythroblasts, respectively. Scale bars: 15  $\mu$ m. (B-C) Cell cycle analysis of the nucleated Ter119<sup>+</sup> erythroblasts in bone marrow of the indicated mice. Statistical analysis of each phase of the cell cycle is shown in (C). N=3 in each group. (D-E) Cell cycle analyses as in (B) and (C) except the experiments were performed in the spleen of the indicated mice. N=3 in each group. (F-G) Nucleated Ter119<sup>+</sup> erythroblasts from bone marrow (F) and spleen (G) of the mDia2<sup>fl/fl</sup>Vav-Cre and control mice were gated for cell cycle analysis as in (B) and (D). Representative plots are presented. (H) Cell cycle analysis was performed on the gated populations from bone marrow, as in Figure 1C. Representative plots of cells from the indicated populations were presented as duplicate in each group. All experiments were repeated at least three times.

genic mice in which Cre recombinase is under the control of the interferon-inducible promoter of the Mx-1 gene.<sup>8</sup> Relative hematopoietic cell-specific mDia2 inducible knockout mice were generated by polyinosinic-polycytidylic acid (poly-I:C) peritoneal injection when the mDia2<sup>fl/fl</sup> Mx-Cre mice were 6 weeks old. mDia2<sup>fl/fl</sup> and mDia2<sup>+/+</sup>Mx-Cre mice with the same poly-I:C injection were used as controls. Ten weeks after poly-I:C injection, the depletion of mDia2 in bone marrow cells was confirmed (Online Supplementary Figure S2A). mDia2<sup>fl/fl</sup> Mx-Cre mice exhibited significant anemia demonstrated by the decreased hemoglobin, total red blood cell count, and hematocrit (Figure 1A and data not shown). Red cell distribution width (RDW) was dramatically increased, reflecting variation of the size of red blood cells (Figure 1A). These changes in red blood cell indices were specific since total white blood cell count remained unchanged (Figure 1A). These results indicate that mDia2 plays a unique role in the erythroid lineage.

We next examined the morphology of the hematopoietic cells from mDia2<sup>fl/fl</sup> Mx-Cre mice. In peripheral blood, these mice exhibited anemia with anisopoikilocytosis

including macrocytes, microcytes, occasional spherocytes, and hypochromic cells, which is consistent with the increased RDW. Polychromasia was relatively increased with abnormally large reticulocytes (Figure 1B). The morphology of granulocytes and lymphocytes from these mice were similar to those from the controls (data not shown). These results indicate that mDia2 could be functionally important to maintain the membrane and cytoskeletal integrity of the mature red blood cells. Additionally, we generated mDia2<sup>fl/fl</sup> Vav-Cre mice that showed the same phenotypes as mDia2<sup>fl/fl</sup> Mx-Cre mice (Online Supplementary Figure S2B).

To determine the etiology of these abnormalities, we analyzed the bone marrow and spleen cells from mDia2<sup>fl/fl</sup> Mx-Cre and control mice 10 weeks after poly-I:C injection. Terminal differentiation of bone marrow CD45 negative erythroid cells was examined using flow cytometric analysis of CD44 surface expression together with forward scatter.<sup>9</sup> In this assay, the CD45 negative erythroid cells were further gated based on their surface levels of CD44, which gradually decreases during cell maturation.<sup>10</sup> As previously reported,<sup>9,10</sup> we divided the

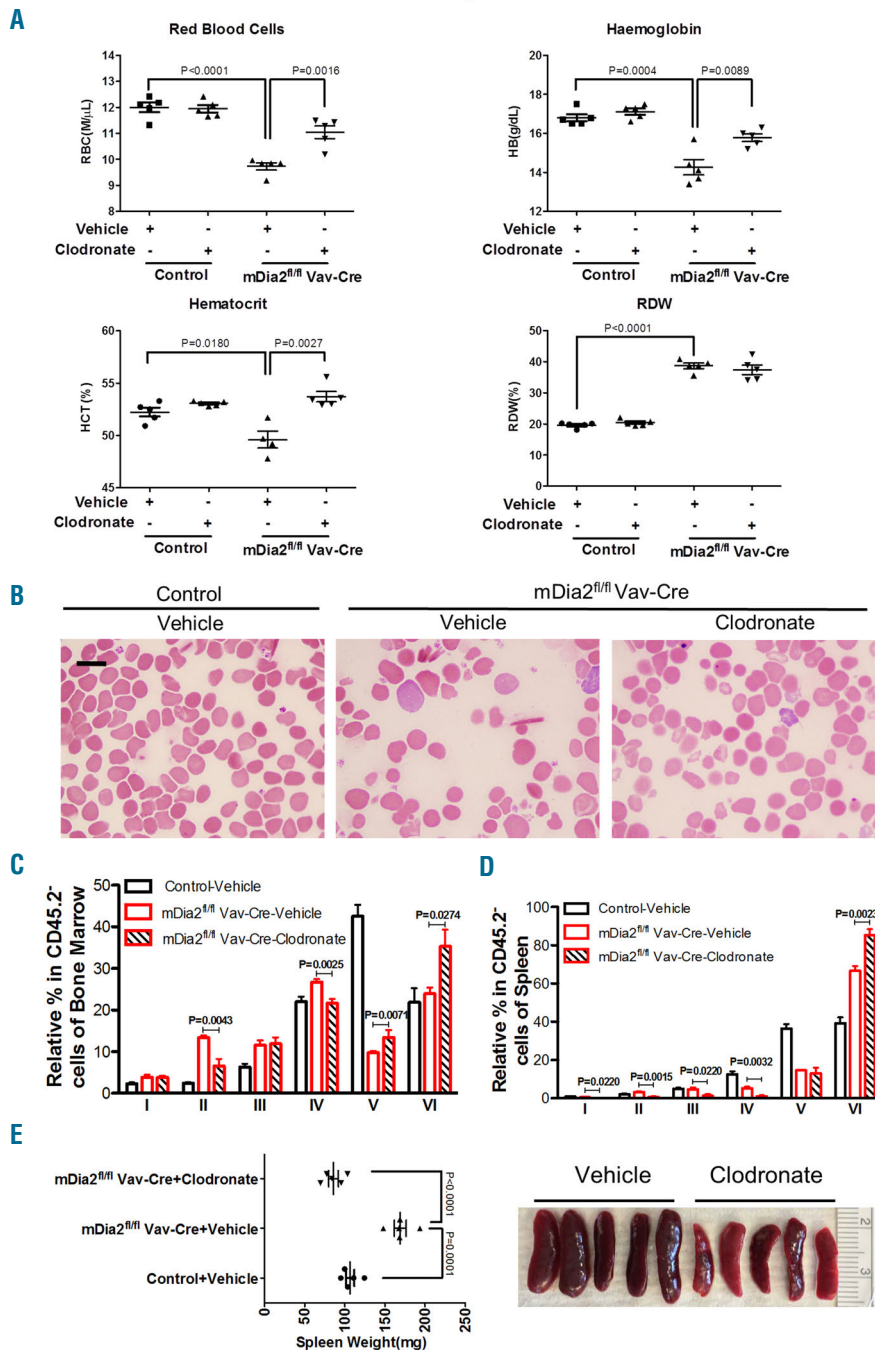


**Figure 3. Macrophage depletion alleviates anemia and ineffective erythropoiesis in mDia2 hematopoietic specific knockout mice.** (A) Eight-week old littermate mice with indicated genotypes were retro-orbitally injected with a single dose of clodronate liposomes (150  $\mu$ l) or vehicle control (Phosphate buffered saline liposomes). Peripheral blood was collected two days after injection and the indicated red blood cell indices were measured using an automated hematology analyzer. (B) Wright-Giemsa stains of peripheral blood smears from indicated mice. Scale bars: 10  $\mu$ m. (C-D) Quantification of populations I-VI from flow cytometric analysis of terminal erythropoiesis in bone marrow (C) and spleen (D) of indicated mice, as in Figure 1C and 1E. N = 5 in each group. (E) Quantification of spleen size of indicated mice (Left). Photographs of spleens of mDia2<sup>fl/fl</sup>Vav-Cre mice treated with vehicle control and clodronate liposomes (Right). N = 5 in each group.

cells into six populations. From the early-stage erythroblasts to more mature forms, populations I to VI represent proerythroblasts, basophilic erythroblasts, polychromatic erythroblasts, orthochromatic erythroblasts, reticulocytes, and mature red blood cells, respectively. Compared to the controls, bone marrow erythroblasts from populations I to III were proportionally increased in mDia2<sup>fl/fl</sup>Mx-Cre mice. In contrast, populations IV to VI, especially population V (reticulocytes), were dramatically decreased (Figure 1C,D). Populations I to III, regarding the spleen, were also proportionally increased. However, populations IV to VI remained relatively stable compared to the controls (Figure 1E,F).

These results reveal that loss of mDia2 in hematopoietic cells causes 1) a significant ineffective erythropoiesis in which most of the erythroid precursors are blocked in the orthochromatic to reticulocyte stages, which is consistent with previous studies stating that mDia2 is critical for enucleation of late-stage erythroblast,<sup>6</sup> and, 2) an extramedullary erythropoiesis in the spleen that compensates ineffective erythropoiesis in bone marrow, which is also demonstrated by the prominent splenomegaly in mDia2<sup>fl/fl</sup>Mx-Cre mice (*Online Supplementary Figure S2C*). We subsequently analyzed the cell survival profiles of the Ter119-positive erythroid cells of bone marrow and spleen of mDia2<sup>fl/fl</sup>Mx-Cre mice. A statistically significant

portion of the erythroid cells in bone marrow, but not in spleen, underwent cell death, although the increase in cell death was relatively small (*Online Supplementary Figure S2D*). We further confirmed the same phenotypes, including increased spleen size and ineffective erythropoiesis in bone marrow and extramedullary erythropoiesis in spleen, in mDia2<sup>fl/fl</sup>Vav-Cre mice (*Online Supplementary Figure S2E and S2G*). Taken together, these data demonstrate that ineffective erythropoiesis contributes to the major pathology of mDia2 hematopoietic specific knockout mice.

To find out the underlying pathology of ineffective erythropoiesis, we compared the morphology of bone marrow cells from mDia2<sup>fl/fl</sup>Mx-Cre and control mice. Strikingly, many erythroblasts in mDia2<sup>fl/fl</sup>Mx-Cre mice were binucleated (*Figure 2A*). Notably, most of the binucleated erythroblasts were in the polychromatic to orthochromatic stages of differentiation. Consistent with the findings in the peripheral blood, no abnormal changes were evident in the myeloid or lymphoid lineages (*Figure 2A*).

To quantify the bi- and multi-nucleated erythroblasts in mDia2<sup>fl/fl</sup>Mx-Cre mice, we labeled the bone marrow cells with DNA staining dye similar to that which is used in cell cycle analysis. In this way, the bi- and multi-nucleated cells would be manifested in and beyond the G2/M phase, respectively. Clearly, the Ter119-positive erythroblasts from both bone marrow (*Figure 2B,C*) and spleen (*Figure 2D,E*) in mDia2<sup>fl/fl</sup>Mx-Cre mice showed a dramatic increase in G2/M phase compared to their counterparts in control mice. The multinucleated erythroblasts were also increased in mDia2<sup>fl/fl</sup>Mx-Cre mice, whereas they were absent in control mice (*Figure 2C and E*). The same increase of binucleated and multinucleated cells was similarly present in mDia2<sup>fl/fl</sup>Vav-Cre mice (*Figure 2F,G*). When analyzed in different developmental stages of terminal erythropoiesis based on CD44 expression in mDia2<sup>fl/fl</sup>Mx-Cre mice (*Figure 1C*), we found that most of the binucleated erythroblasts were in stage IV orthochromatic phase of differentiation in bone marrow (*Figure 2H*). This is consistent with the morphologic findings (*Figure 2A*).

To further understand the mechanism of mDia2 in erythropoiesis, we used a well established mouse erythroblasts *in vitro* differentiation system.<sup>11-15</sup> Compared to the controls, the lineage-negative cells from mDia2<sup>fl/fl</sup>Mx-Cre mice showed significantly decreased proliferation, differentiation, and enucleation (*Online Supplementary Figure S3A, S3B, and S3C, respectively*). Morphologic analysis of the erythroid cells with loss of mDia2 revealed frequent binucleated and enucleating cells (*Online Supplementary Figure S3D*), further confirming the *in vivo* assays and the cell-autonomous defects. These binucleated cells are mostly present in Ter119-positive erythroblasts but not in the Ter119-negative cells, and appeared at the late stages of terminal differentiation, at 48 hours or 72 hours (*Online Supplementary Figure S3E and S3F*), again confirming the *in vivo* findings.

We thereafter attempted to rescue anemia in mDia2 deficient mice. Previous reports showed that macrophages contribute to the pathogenesis of ineffective erythropoiesis in beta-thalassemia<sup>14,15</sup>. The depletion of macrophages by a single dose of clodronate significantly improves anemia in beta-thalassemia mouse models.<sup>14</sup> We therefore treated these mice similarly with a single dose of clodronate, followed by a complete blood count and blood smear examination. This treatment led to a significant improvement of anemia as indicated by increased red blood cell counts, hemoglobin levels and

hematocrit (*Figure 3A,B*). We confirmed the depletion of macrophages in bone marrow (*Online Supplementary Figure S4A and S4B*). Bone marrow examination also showed that clodronate reduced the percentage of early-stage erythroblasts, whereas reticulocytes and red blood cells (populations V and VI, respectively) were significantly increased (*Figure 3C*). Although spleen already showed compensation in mDia2 conditional knockout mice (*Online Supplementary Figure S2G*), clodronate treatment further reduced the early-stage ineffective erythroblasts (*Figure 3D*). Consistently, the improved erythropoiesis in bone marrow and spleen led to a normalized spleen weight (*Figure 3E*). These results further demonstrate the therapeutic effects of macrophage depletion in the treatment of ineffective erythropoiesis.

In summary, our study reveals the key roles of mDia2 in adult terminal erythropoiesis. Loss of mDia2 affects terminal erythropoiesis particularly in the orthochromatic stage by compromising cytokinesis and enucleation of the condensed nuclei. This leads to the inhibition of differentiation of the early-stage erythroblasts. These pathologic features closely mimic certain inherited diseases in humans, such as congenital dyserythropoietic anemia, which indicates that mDia2 may play a role in its pathogenesis. Additionally, the mDia2 conditional and tissue-specific knockout mouse models also provide tools with which to study the functions of mDia2 in different organ systems.

Yang Mei,<sup>1</sup> Baobing Zhao,<sup>1</sup> Jing Yang,<sup>1</sup> Juehua Gao,<sup>1</sup> Amittha Wickrema,<sup>2</sup> Dehua Wang,<sup>3</sup> Yihua Chen,<sup>1</sup> and Peng Ji<sup>1</sup>

<sup>1</sup>Department of Pathology, Feinberg School of Medicine, Northwestern University, Chicago, IL; <sup>2</sup>Section of Hematology/Oncology, Department of Medicine, The University of Chicago, IL; and <sup>3</sup>Division of Pathology and Laboratory Medicine, Cincinnati Children's Hospital Medical Center, OH, USA

*Funding:* the work is supported by a Pathway to Independence award from National Institute of Health (R00HL102154) and an American Society for Hematology (ASH) scholar award to PJ.

*Acknowledgments:* the authors thank Drs. Jing Zhang and John Crispino for helpful discussion, Dr. Lynn Doglio of the Transgenic and Targeted Mutagenesis Laboratory of Northwestern University for the help of generating mDia2 conditional knockout mice, Dr. Lin Li of the Mouse Histology and Phenotyping Laboratory of Northwestern University for the help with mouse histology.

*Correspondence:* ji.peng@northwestern.edu  
doi:10.3324/haematol.2015.134221

*Key words:* mDia2, erythropoiesis, cytokinesis, enucleation, knockout mice.

*Information on authorship, contributions, and financial & other disclosures was provided by the authors and is available with the online version of this article at [www.haematologica.org](http://www.haematologica.org).*

## References

- Hattangadi SM, Wong P, Zhang L, Flygare J, Lodish HF. From stem cell to red cell: regulation of erythropoiesis at multiple levels by multiple proteins, RNAs, and chromatin modifications. *Blood*. 2011;118(24):6258-6268.
- Ji P, Murata-Hori M, Lodish HF. Formation of mammalian erythrocytes: chromatin condensation and enucleation. *Trends Cell Biol*. 2011;21(7):409-415.
- Ji P. New Insights into the Mechanisms of Mammalian Erythroid Chromatin Condensation and Enucleation. Elsevier Ltd; 2015.
- Keerthivasan G, Wickrema A, Crispino JD. Erythroblast enucleation. *Stem Cells Int*. 2011;2011:139851.
- Faix J, Grosse R. Staying in shape with formins. *Dev Cell*. 2006;10(6):693-706.
- Ji P, Jayapal SR, Lodish HF. Enucleation of cultured mouse fetal ery-

- throblasts requires Rac GTPases and mDia2. *Nat Cell Biol.* 2008; 10(3):314-321.
7. Watanabe S, De Zan T, Ishizaki T, et al. Loss of a Rho-Regulated Actin Nucleator, mDia2, Impairs Cytokinesis during Mouse Fetal Erythropoiesis. *Cell Reports.* 2013;5(4):926-932.
  8. Kühn R, Schwenk F, Aguet M, Rajewsky K. Inducible gene targeting in mice. *Science.* 1995;269(5229):1427-1429.
  9. Liu J, Zhang J, Ginzburg Y, et al. Quantitative analysis of murine terminal erythroid differentiation in vivo: novel method to study normal and disordered erythropoiesis. *Blood.* 2013;121(8):e43-9.
  10. Liu J, Mohandas N, An X. Membrane assembly during erythropoiesis. *Curr Opin Hematol.* 2011;18(3):133-138.
  11. Zhang J, Socolovsky M, Gross AW, Lodish HF. Role of Ras signaling in erythroid differentiation of mouse fetal liver cells: functional analysis by a flow cytometry-based novel culture system. *Blood.* 2003;102(12):3938-3946.
  12. Socolovsky M, Fallon AE, Wang S, Brugnara C, Lodish HF. Fetal anemia and apoptosis of red cell progenitors in Stat5a<sup>-/-</sup>5b<sup>-/-</sup> mice: a direct role for Stat5 in Bcl-X(L) induction. *Cell.* 1999;98(2):181-191.
  13. Shuga J, Zhang J, Samson LD, Lodish HF, Griffith LG. In vitro erythropoiesis from bone marrow-derived progenitors provides a physiological assay for toxic and mutagenic compounds. *Proc Natl Acad Sci USA.* 2007;104(21):8737-8742.
  14. Ramos P, Casu C, Gardenghi S, et al. Macrophages support pathological erythropoiesis in polycythemia vera and  $\beta$ -thalassemia. *Nat Med.* 2013;19(4):437-445.
  15. Chow A, Huggins M, Ahmed J, et al. CD169<sup>+</sup> macrophages provide a niche promoting erythropoiesis under homeostasis and stress. *Nat Med.* 2013;19(4):429-436.